



Published in final edited form as:

*Ann Surg.* 2020 July ; 272(1): 183–193. doi:10.1097/SLA.0000000000003172.

## Doxycycline Reduces Scar Thickness and Improves Collagen Architecture

Alessandra L. Moore, MD<sup>\*,†</sup>, Heather E. desJardins-Park, AB<sup>\*</sup>, Bryan A. Duoto, BS<sup>#</sup>, Shamik Mascharak, BS<sup>#</sup>, Matthew P. Murphy, MB, BCh, BAO, MRCSI<sup>\*</sup>, Dre M. Irizarry, MD<sup>\*</sup>, Deshka S. Foster, MD<sup>\*</sup>, Ruth E. Jones, MD<sup>\*</sup>, Leandra A. Barnes, AB<sup>#</sup>, Clement D. Marshall, MD<sup>#</sup>, Ryan C. Ransom, BS<sup>\*,‡</sup>, Gerlinde Wernig, MD<sup>§</sup>, Michael T. Longaker, MD, MBA, FACS<sup>\*,‡</sup>

<sup>\*</sup> Department of Surgery, Stanford University School of Medicine, Stanford, CA

<sup>†</sup> Department of Surgery, Brigham and Women's Hospital, Boston, MA

<sup>‡</sup> Stanford Institute for Stem Cell Biology and Regenerative Medicine, Stanford, CA

<sup>§</sup> Department of Pathology, Stanford University School of Medicine, Stanford, CA.

<sup>#</sup> These authors contributed equally to this work.

### Abstract

**Objective:** To investigate the effects of local doxycycline administration on skin scarring.

**Background:** Skin scarring represents a major source of morbidity for surgical patients. Doxycycline, a tetracycline antibiotic with off-target effects on the extracellular matrix, has demonstrated antifibrotic effects in multiple organs. However, doxycycline's potential effects on skin scarring have not been explored in vivo.

**Methods:** Female C57BL/6J mice underwent dorsal wounding following an established splinted excisional skin wounding model. Doxycycline was administered by local injection into the wound base following injury. Wounds were harvested upon complete wound closure (postoperative day 15) for histological examination and biomechanical testing of scar tissue.

**Results:** A one-time dose of 3.90mM doxycycline (2mg/mL) within 12 hours of injury was found to significantly reduce scar thickness by 24.8% ( $*P < 0.0001$ ) without compromising tensile strength. The same effect could not be achieved by oral dosing. In doxycycline-treated scar matrices, collagen I content was significantly reduced ( $*P = 0.0317$ ) and fibers were favorably arranged with significantly increased fiber randomness ( $*P = 0.0115$ ). Common culprits of altered wound healing mechanics, including angiogenesis and inflammation, were not impacted by

---

Requests for reprints should be addressed to the corresponding author Michael T. Longaker, MD, MBA, FACS, Hagey Laboratory for Pediatric Regenerative Medicine, Stanford University, 257 Campus Drive, Stanford, CA 94305. Longaker@stanford.edu.

Supplemental digital content is available for this article. Direct URL citations appear in the printed text and are provided in the HTML and PDF versions of this article on the journal's Web site ([www.annalsurgery.com](http://www.annalsurgery.com)).

The authors report no conflicts of interest.

A.L.M. designed experiments. A.L.M., H.E.dJ-P, B.A.D., S.M., M.P.M. analyzed data. A.L.M., H.E.dJ-P, B.A.D., D.S.F., R.E.J., S.M., M.P.M., D.M.I., C.D.M., L.A.B., R.C.R. performed experiments. A.L.M., H.E.dJ-P, B.A.D., S.M., M.P.M., G.W., M.T.L. wrote and edited the manuscript.

doxycycline treatment. However, *engrailed1* profibrotic fibroblasts, responsible for scar extracellular matrix deposition, were significantly reduced with doxycycline treatment (\* $P=0.0005$ ).

**Conclusions:** Due to the substantial improvement in skin scarring and well-established clinical safety profile, locally administered doxycycline represents a promising vulnerary agent. As such, we favor rapid translation to human patients as an antiscarring therapy.

## Keywords

fibrosis; scarring; wound healing

Skin scarring is a major source of morbidity for surgical patients. Each year, more than 70 million surgical incisions are created in the United States alone.<sup>1</sup> Up to 70% of surgical scars will become hypertrophic or more rarely will form keloids.<sup>2</sup> Additionally, when injuries cause significant soft tissue destruction, scars can form contractures that severely disable patients by immobilizing joints. For these reasons, it is well understood that scars can severely impact the functional status and psychological well-being of patients.<sup>3</sup> Because skin scarring leads to both cosmetic and functional tissue compromise, an estimated \$25 billion US is spent annually on skin scarring products, scar revision, and wound healing.<sup>1</sup>

Doxycycline is a well-known tetracycline antibiotic that functions as a ribosome 30S subunit inhibitor, but also has off-target effects.<sup>4,5</sup> Several reports document the potential vulnerary effects of doxycycline in the eye,<sup>6</sup> in the oral cavity,<sup>7,8</sup> and following hernia repair<sup>9</sup> and imply an ability to reduce skin scarring.<sup>10–12</sup> Here, we report that a one-time local dose of 3.90 mM doxycycline (2 mg/mL) within 12 hours of injury significantly reduces scar thickness without compromising tensile strength. The same effect cannot be achieved by oral dosing. Skin wounds treated with doxycycline exhibit favorable collagen patterning, likely driven by a reduction in *engrailed1*-positive skin fibroblasts, which deposit the majority of scar extracellular matrix.

## METHODS

### Mice

Mice were housed and maintained per Stanford University guidelines in sterile microinsulators. Food and water were provided ad libitum. *En1<sup>tm2(cre)W<sup>1st</sup></sup>* (*En1<sup>Cre/-</sup>*), B6.Cg-*Commd10<sup>Tg(Vav1-icre)</sup>A2Kio* (*Vav1<sup>Cre/-</sup>*), B6.129(Cg)-*Gt(ROSA)26Sor<sup>tm4(CTB-tdTomato,-EGFP)Luo</sup>* (*Rosa26<sup>mTmG/mTmG</sup>*), and C57BL/6J mice were purchased from Jackson Laboratories (Bar Harbor, ME). *En1<sup>Cre/-</sup>* and *Vav1<sup>Cre/-</sup>* mice were bred to *Rosa26<sup>mTmG/mTmG</sup>* reporter mice to generate heterozygous offspring with membrane-bound tomato red fluorescent protein (mRFP) labeled tissues and Cre-recombinant membrane-bound green fluorescent protein (mGFP) labeled reporter cells (Supplemental Figure 1A, <http://links.lww.com/SLA/B552>).

### Splinted Excisional Skin Wounding

Eight- to 12-week-old transgenic and C57BL/6J animals underwent skin wounding as previously described.<sup>13</sup> This method employs a dorsal splint to prevent wound contraction

and mimic human wound healing kinetics (Supplemental Figure 1B, <http://links.lww.com/SLA/B552>). In brief, animals were anesthetized with 1% to 2% isoflurane/oxygen. Dorsal fur was removed, and skin was sterilized with 70% ethanol. Full-thickness skin wounds, 6 mm in diameter, were placed through the panniculus carnosus using a combination of dermal biopsy punches and surgical scissors. Two symmetric wounds were created per animal. A circular 12 mm diameter silicone splint (Invitrogen) was then fixed to the skin using adhesive (Krazy Glue, West Jefferson, OH) and 8 evenly spaced 6–0 nylon sutures (Ethicon). For topical wound treatments, doxycycline hyclate (Sigma-Aldrich) was resuspended in phosphate-buffered saline (PBS, Gibco) at a concentration of 0.1 mg/mL, 2mg/mL, or 20mg/mL, and 30  $\mu$ L of doxycycline or PBS were injected into the base of the wound bed at various time points [time = T0 (immediately after surgery) or T12, 24, or 48h after surgery]. Tetracycline and minocycline solutions (Sigma-Aldrich) at 2 mg/mL were injected in the same manner (n = 10 wounds per treatment group). Skin wounds were then dressed with Tegaderm (3M) which was replaced every other day until wound harvest. Wounds were harvested on postoperative day 15 (healed, n = 10 wounds per group) for wound healing analysis and on postoperative days 0,5,9, and 14 (n = 6 wounds per group per day) for fluorescence-activated cell sorting (FACS). Transgenic animal experiments were performed on n = 3 animals (n = 6 wounds) per group. Delayed doxycycline administration (T0, 12, 24, and 48 h postoperative) was performed on n = 4 wounds per group. For *per ora* (PO) doxycycline administration (n = 10 wounds per group), doxycycline was suspended in dietary drinking water at a concentration of 2 mg/mL.

### Tissue Processing and Staining

Harvested tissue was fixed in 10% buffered formalin phosphate (Fisher Chemical) for 16 to 18hours at 4°C. For traditional histologic stains (hematoxylin and eosin, trichrome, picrosirius red), tissue was embedded in paraffin per standard protocols and cut into 8 mm thick sections using a Leica RM2255 microtome. Samples were stained with hematoxylin and eosin (Sigma-Aldrich), Masson's Trichrome Kit (Sigma-Aldrich), or the Picro Sirius Red Stain Kit (Abcam) by manufacturer's protocols.

### Quantification of Scar Thickness

Hematoxylin and eosin-stained slides were imaged with a Leica DMI4000B inverted scope using bright field at  $\times 10$  magnification to capture the entire scar area. Dermal thickness was measured using the linear measuring tool on Adobe Photoshop CS6. Measurements were performed by a blinded reviewer then analyzed using a Mann-Whitney *U* test. After completely sectioning through the scar specimens, 2 representative slides from the proximal, middle, and distal third of each specimen were selected for staining. Each slide contained 3 tissue sections, each adjacent to one another within the same third of the tissue specimen. After staining, the scar thickness was estimated by separating each stained specimen into 2 lateral and a middle third, and then measuring the scar depth at the center of each third. This allowed for an estimation of the scar depth and normalized for any inconsistencies in scarring and wounding between specimens. A total of 5 mice were used per group for a total of n = 10 wounds per group.

### Tensile Strength Testing

Tensile strength testing was performed as previously described without modifications.<sup>14</sup> In brief, healed (postoperative day 15) wounds were harvested, and scar strength was assessed using a microtester (Instron, model 5848) equipped with a 100-N load cell. Custom grips with double-sided adhesive tape were used to attach skin specimens and permit stretching until breakage. Breakage was detected by a sudden decrease in stress as strain increased. Analysis was performed as previously described<sup>15</sup> using MATLAB (Math-works) software, giving values for true strain, true stress, and finally tensile strength.

### Quantification of Wound Healing Rate

After wounding, wounds were imaged immediately and every other day using an iPhone 8 Plus (Apple). Images were analyzed as previously published.<sup>14</sup> Wound healing was measured by the advancement of keratinocytes over the wound bed until closure was achieved (day 15), by measuring wound circumference using the Adobe Photoshop CS6 magnetic lasso tool. The rate of wound healing was calculated as a percent of the original wound size over time. Significant differences between group means were calculated using an Analysis of Variance followed by Mann-Whitney *U* test for each postoperative day and group pairing.

### Assessment of Bacterial Contamination

Wounds treated with PBS or 2 mg/mL doxycycline were assessed for bacterial contamination on postoperative days 1, 3, 5, 7, and 9 (n = 10 wounds). Wound bases were swabbed with a sterile P200 pipette tip and the swabbed specimen was transferred to petri dishes containing LB Broth with agar (Lennox Formula, Sigma Aldrich) without antibiotics. Each plate contained pooled wound contamination from a single mouse, for n = 5 plates per group per time point. Cultures were maintained in an Isotemp (Fisher Scientific) dry incubator at 38°C for 24 hours before imaging with an Epson Perfection V600 Photo Scanner. A human buccal swab was utilized as a positive control. Colonies were manually counted, then compared using a Student *t* test.

### Immunostaining of Tissue Specimens

For immunofluorescent staining and quantification of endogenous fluorescence, tissue was soaked in 30% sucrose/PBS for 2 weeks at 4°C then embedded in Tissue Tek Optimal Cutting Temperature Compound (OCT, Sakura Fintek). Frozen blocks were cut into 8 μm thick sections using a CryoStar NX70 cryostat (Thermo Scientific). Immunostains were performed by standard protocols without modifications. In brief, slides were cleared using PBS. For nuclear and intracellular stains, cells were permeabilized with 0.1% Triton-X (Sigma-Aldrich) in PBS for 20 minutes. Specimens were then blocked for 30 minutes using 1:10 PowerBlock (BioGenex, Fremont, CA) in PBS, followed by application of primary antibodies at concentrations per their product specifications for 1 hour. Specimens were washed with PBS 3 times before application of secondary antibodies at concentrations per their product specifications for 1 hour. After washing 3 times with PBS, slides were mounted using a 4',6-diamidino-2-phenylindole (DAPI) containing mounting medium (Fluoroshield Mounting Medium with DAPI, Abcam) and glass coverslips. Slides were kept at 4°C until

imaging within 24 to 48 hours. Antibodies are listed in Supplemental Table 1, <http://links.lww.com/SLA/B552>.

### Fluorescence Quantification

To quantify collagen deposition, histological sections of scars were stained with Masson trichrome or Picrosirius Red and imaged ( $\times 40$  objective) by brightfield microscopy on a Leica DMI 4000B inverted microscope or polarization microscopy on a Leica DFC9000 GT inverted microscope, respectively. Next, color deconvolution was performed in Fiji (ImageJ, NIH) to isolate blue collagen fibers in trichrome sections or red (mature) and green (immature) fibers in Picrosirius Red sections. Mean gray intensity was measured as a surrogate of overall collagen content. The Image Processing Toolbox in Matlab 2017a was utilized for characterization of individual collagen fibers and collagen networks.

Deconvoluted Picrosirius Red images corresponding to mature and immature fibers were denoised by processing through an adaptive Wiener filter (*wiener2* Matlab function, 3-by-3 neighborhoods). Images were then brightness-adjusted (*imadjust*) to optimize contrast and converted into binary maps of fibers and background (*im2bw*). Next, the binary maps were eroded by a diamond-shaped structuring element (*imerode*), dilated by a line structuring element, and then eroded again; these steps served to remove nonlinear elements. Finally, binary maps were “skeletonized” using the *bwmorph* function, thereby producing continuous traces of individual collagen fibers and branch-points. A schematic of the image processing technique is represented in Figure 4E. From the skeletonized map, a variety of fiber characteristics such as length, width, persistence, and major/minor axes were automatically quantified using the *regionprops* function. To quantify the randomness of fiber networks, orientations measured using *regionprops* were fit to the von Mises distribution (a circular analogue of the normal distribution) and the constant value  $\kappa$  was calculated using the Circular Statistics Toolbox (credit: Philipp Berens). Lower  $\kappa$  values indicate greater randomness in the underlying fiber orientations; “fiber randomness” is reported as the inverse of  $\kappa$  ( $\kappa^{-1}$ ). Image processing tools in Matlab 2017a were also used to automate the characterization of blood vessels. First, CD31-stained histological sections were imaged by confocal microscopy on a Leica SP5 multiphoton upright confocal microscope and converted to max projections in Fiji. Next, images were processed through a Frangi filter, which can be used to detect continuous edges such as those in blood vessels (credit: Dirk-Jan Kroon), and then converted to binary maps of vessels and background. Further processing (erosion, dilation, skeletonization, etc.) and quantification steps were identical to those used for collagen fiber quantification, but erosion was performed only once.

### Preparation of Cells for Fluorescence Activated Cell Sorting (FACS)

Preparation of animal tissue for FACS was performed as previously described.<sup>16</sup> In brief, wounds were harvested ( $n = 6$  wounds per timepoint) and minced with fine scissors before adding to 0.5mg/mL Liberase DL (Sigma-Aldrich) in Dulbecco’s modified Eagle Medium (DMEM, Gibco), then incubated at 37°C for 30 minutes. After digestion, enzyme was quenched by addition of media containing 20% fetal bovine serum (FBS, Gibco), and tissue was strained through a 100  $\mu\text{m}$  followed by a 40  $\mu\text{m}$  strainer to achieve a single cell suspension. Cells were incubated with pre-conjugated antibodies for 30 minutes in PBS with 1% FBS, 0.1% penicillin/ streptomycin (P/S, Gibco), and 1 mM ethylenediaminetetraacetic

acid (Invitrogen). Antibodies are listed in Supplemental Table 2, <http://links.lww.com/SLA/B552>. Cells were washed with PBS to remove antibodies in solution before performing flow cytometry.

### Flow Cytometry and FACS Analysis of Resident Inflammatory Cell Populations

Fluorescence compensation was performed to correct any spectral overlap. Propidium iodide (PI) was added to samples at 1 mg/mL as a viability assay. Fluorescence minus one samples were run first to establish gating strategy for sorting. The following panels were used for sorting: 1) SSC-A versus FSC-A to capture all cells; 2) FSC-W versus FSC-H to capture singlets; 3) SSC-W versus SSC-H to capture singlets; 4) PI versus CD45-PECy5 (eBioscience, cat. no 15–0451-82) to capture all live (PI-), hematopoietic (CD45+) cells; 5) B220-PE (eBioscience, cat. no 12–0452-82) versus MAC1-BV421 (BD Horizon, cat. no 560456) to capture 3 populations: B-cells (B220+), macrophages (MAC1+), lymphocytic populations (B220– MAC1–). Representative FACS plots are shown in Figure 5A.

### Statistics

Preparation of text and numeric files was performed using Microsoft Excel. Statistical analyses including analysis of variance, Mann-Whitney *U* test, Wilcoxon Rank Sum Test, and Student *t* test, were performed using GraphPad Prism version 6.0c. Results were presented as the mean  $\pm$  the standard error of the mean. Alpha values were 0.05 for all experiments, and a *P* value of less than 0.05 was considered statistically significant.

## RESULTS

### Doxycycline Reduces Scar Thickness Without Sacrificing Tensile Strength

Female C57BL/6J mice underwent dorsal splinted excisional wounding via an established protocol which prevents rapid wound contraction and results in human-like wound healing kinetics.<sup>13</sup> The mice received a 30  $\mu$ L wound base injection of PBS or 0.1, 2, or 20 mg/mL doxycycline immediately following surgery (time, T0), and scars were harvested upon complete wound closure (day 15) for scar thickness assessment by histological examination. Scar thickness was significantly reduced in the 2mg/mL [24.8% reduction compared with control (PBS), \**P* < 0.0001] and 20mg/mL (18.0% reduction, \**P* = 0.0023) dosage groups (Fig. 1A, B). Reduced scar thickness correlated with significantly reduced total collagen as assessed by Masson trichrome stain in the 0.1mg/mL (\**P* = 0.0357) and 2mg/mL (\**P* = 0.0317) treatment groups, but not at 20mg/mL (*P* = 0.3968) (Fig. 1C, D). This could be explained by the fact that at 20 mg/mL, doxycycline has reached a concentration of 39.0 mM and may be acting via acid/base chemistry on the tissue at this concentration rather than as a direct inhibitor or promoter of cellular/enzyme activity.<sup>17</sup> Thus, the mechanism of reduced scar thickness at 20mg/mL may be different than at a dose of 2mg/mL. Based on these data, local doxycycline treatment at a dosage of 2 mg/ mL displayed the most consistent improvement in scarring, and as such further experiments were performed at this concentration. Though scar thickness and total collagen were significantly reduced with local doxycycline, tensile strength was not significantly compromised (*P* = 0.4376) in the 2mg/mL local doxycycline treatment group (Fig. 1E, F). Additionally, time to wound closure was not adversely influenced by doxycycline treatment (Fig. 2A).

## Local Versus Systemic Effects of Doxycycline

Because 2 wounds were created on each animal (Supplemental Figure 1B, <http://links.lww.com/SLA/B552>), we questioned whether treatment of 1 wound with doxycycline would be sufficient to positively influence scarring in the contralateral wound. To test this hypothesis, the right dorsal wound of each mouse was injected with 2 mg/mL doxycycline and the left wound was treated with PBS. No statistically significant difference in scar thickness was observed ( $P = 0.6257$ ) using a paired analysis between left and right wounds of mice treated in this manner (Fig. 2B). This finding suggests that doxycycline injected locally into 1 wound is able to favorably influence scarring in both the doxycycline-treated wound and the contralateral (control-treated) wound. This may be related to the ready lipid solubility of doxycycline.<sup>18</sup> Alternatively, this result could highlight the possibility that doxycycline may be influencing scar thickness via systemic circulation. To address this possibility, we then questioned whether oral delivery of doxycycline would also induce a positive effect on scarring. However, when doxycycline was dosed PO, the resultant scar thickness was not significantly reduced ( $P = 0.3006$ ) compared with scars following control treatment (local PBS injection only) (Fig. 2C).

## Type of Tetracycline Antibiotic and Timing of Injection Matters

Given the dramatic reduction in scar thickness with local doxycycline administration, other commonly used tetracycline antibiotics (minocycline and tetracycline) were also evaluated. With minocycline and tetracycline treatment, a detrimental impact on wound healing was observed, with significantly increased scar thickness in both treatment groups (minocycline  $*P < 0.0001$ , tetracycline  $*P < 0.0001$ ) compared with PBS controls (Fig. 3A). We also considered whether timing of antibiotic administration influenced the vulnerability of local doxycycline. As the time between initial injury and local doxycycline injection was increased (time = T0, 12, 24, and 48 h postoperative), mean scar thickness also increased (Fig. 3B). When doxycycline was administered 48 hours postoperatively, there was no significant difference in resultant scar thickness, though variability increased (Fig. 3B). These results imply a mechanism of action that is limited to doxycycline rather than common to all tetracyclines and that is also time sensitive, where reduced scar thickness is only accomplished with early (<12h after incision) administration.

## Local Doxycycline Does Not Impact Wound Contamination

To evaluate the mechanism of reduced scar thickness with local doxycycline treatment, we first considered whether this effect was mediated by reduced wound contamination secondary to doxycycline's antimicrobial effects. However, cultured wound swabs showed no significant difference in wound contamination ( $P > 0.2328$ , all timepoints) between the control and 2mg/mL doxycycline treatment groups (Supplemental Figure 1C, <http://links.lww.com/SLA/B552>). Notably, contamination was minimal in the excisional skin wounds overall (0–26 colony forming units), consistent with prior publications suggesting that significant bacterial contamination in mouse wounds requires inoculation.<sup>19–21</sup>

## Doxycycline Increases Scar Collagen Branching and Randomness

Despite having increased collagen content compared with healthy skin, skin scars never achieve the same tensile strength as unwounded skin due to the tight parallel alignment of scar collagen bundles.<sup>22</sup> Rather, the tensile strength of unwounded skin is due to the “basketweave” orientation of collagen in the dermis that allows both flexibility and pliability.<sup>22</sup> To understand the mechanism behind preserved tensile strength in the setting of reduced scar collagen in doxycycline treated skin wounds, healed tissue was assessed using a Picosirius Red stain for collagen quantity and structure. Picosirius Red has the advantage of delineating mature (red, Picro Red) and immature (green, Picro Green) collagen fibers,<sup>23</sup> which may correlate with type I and type III collagen, respectively.

In the Picro Red fibers, which represent mature collagen, there was a significant decrease in relative intensity ( $*P=0.0042$ ) in the 2mg/mL group compared with PBS controls (Fig. 3C, top panel; Fig. 3D). This finding correlated with a significant reduction in anti-collagen I immunostaining ( $*P=0.0430$ ) (Fig. 3E, F). Picro Red fibers also displayed decreased fiber number ( $*P=0.0098$ ) and length ( $*P=0.0226$ ) in the 2 mg/mL treatment group (Fig. 4A, B, left panels). Picro Red fiber branching was reduced with 0.1 mg/mL ( $*P=0.0159$ ) and 2 mg/mL ( $*P=0.0053$ ) but increased with 20 mg/mL ( $*P=0.0009$ ) treatment (Fig. 4C, left panel). However, Picro Red fiber randomness was significantly increased with both 2 mg/mL ( $*P=0.0115$ ) and 20 mg/mL ( $*P=0.0282$ ) treatment (Fig. 4D, left panel). A schematic of the image deconvolution technique, which involved automated image processing using MATLAB to permit individual fiber analysis, is represented in Figure 4E.

Interestingly, Picro Green fibers, which represent immature collagen, showed a significant increase in fiber intensity (0.1 mg/mL  $*P=0.0441$ , 2 mg/mL  $*P=0.0114$ ) (Fig. 3C, bottom panel; Fig. 3D). This correlated with an increased number of Picro Green fibers (0.1 mg/mL  $*P=0.0292$ ) (Fig. 4A, right panel). Picro Green fiber length, however, was not affected ( $P>0.1357$ , all dosages) by doxycycline (Fig. 4B, right panel). Additionally, Picro Green fibers exhibited significantly increased branching (2 mg/mL  $*P=0.0444$ ) and randomness (20 mg/mL  $*P=0.0289$ ) (Fig. 4C, D, right panels). Overall, these data suggest that the orientation of collagen in doxycycline treated wounds more closely resembles the more branched, randomly aligned collagen of unwounded skin.

## Doxycycline Does Not Impact Inflammatory Cell Recruitment

Inflammation is another important aspect of wound healing. Neutrophils, macrophages, mast cells, and other inflammatory cells are recruited to wound beds to both sanitize the area and stimulate local skin cells to form granulation tissue and re-epithelialize.<sup>22</sup> To assess whether inflammatory cell recruitment was altered in doxycycline treated wounds, splinted excisional skin wounds were created on the dorsa of *Vav1<sup>Cre</sup>;**Rosa26<sup>mTmG</sup>*<sup>-/-</sup> mice, which express GFP on hematopoietic lineage cells and express RFP on all other tissues. Our results showed no significant difference in inflammatory cell recruitment in 2 mg/mL doxycycline treated wounds ( $P=0.2970$ ) compared with PBS controls (Supplemental Figure 2A–B, <http://links.lww.com/SLA/B552>). We then performed FACS to delineate the number and proportion of different inflammatory cell populations. When FACS was performed on wounds at T12hours and at 5, 9, and 14 days postoperative, there was no significant



difference ( $P > 0.1000$ ) in the relative proportion of recruited B cells (B220+) and T cells (B220- MAC1-) (Fig. 5A, B). At postoperative day (POD) 9 there was a significant increase ( $*P = 0.0407$ ) in macrophages, which are known to influence collagen remodeling, in the doxycycline treated group, but this was not observed at other time points (Fig. 5B).

### Doxycycline Does Not Impact Angiogenesis

Expedited wound closure in chronic wounds and improvements in wound healing quality have previously been linked to augmented angiogenesis.<sup>24,25</sup> To evaluate whether doxycycline improves wound healing by influencing angiogenesis, skin wounds from *Vav1<sup>Cre</sup><sup>-/-</sup>;Rosa26<sup>mTmG</sup><sup>-/-</sup>* mice were stained for CD31 to identify endothelial cells within the wound base. In doxycycline treated wounds, there was a trend toward, but no significant increase in, blood vessels in treated wound beds as compared with controls (Supplemental Figure 2C–D, <http://links.lww.com/SLA/B552>).

### Doxycycline Reduces En1+ Fibroblasts in Skin Scars

Scar tissue deposition, whether influenced by inflammatory cells or endothelial cells, is ultimately dependent on the action of skin fibroblasts. Recently, our group reported the discovery of a dermal fibroblast lineage, defined by expression of *engrailed1* (*En1*), which deposits the vast majority of skin scar collagen in mouse dorsal wounds.<sup>16</sup> Additionally, the same cells can be identified in human scars using the cell surface marker CD26.<sup>26</sup> Given the importance of En1-positive fibroblasts (EPFs) in scar formation, splinted excisional wounds were created on the dorsa of *En1<sup>Cre</sup><sup>-/-</sup>;Rosa26<sup>mTmG</sup><sup>-/-</sup>* mice and mice were randomized to receive PBS or 2 mg/mL doxycycline wound injections. Upon complete wound closure (POD 15), wounds were harvested and imaged using confocal microscopy. Results revealed a significant reduction in EPFs, identified by a significant relative decrease in GFP intensity ( $*P = 0.0005$ ), in doxycycline treated skin wounds (Fig. 6A, B). As mentioned previously, EPFs are responsible for the vast majority of extracellular matrix deposition to create scars during adult wound repair.<sup>16</sup> Thus, the significant decrease in EPFs observed in doxycycline-treated wounds may explain both the overall reduction and the structural alteration in scar collagen.

## DISCUSSION

Despite the significant clinical burden as well as the substantial consumer market associated with scarring, very few truly effective antiscarring therapies exist which reduce scar burden while maintaining skin mechanical strength. While doxycycline's ability to reduce fibrosis in other organs has been suggested by previous studies,<sup>6–9</sup> its potential effects on skin scarring had heretofore remained unexplored. Through this series of experiments, we demonstrate for the first time the potent ability of doxycycline to reduce scar thickness without compromising scar tensile strength.

Our data suggest a promising structure of collagen fibers in the extracellular matrix of doxycycline-treated wounds that more closely resembles the branched, randomly aligned “basketweave” pattern of collagen deposition in unwounded skin. This more normal appearing collagen structure may explain the finding of preserved scar strength in the face of

reduced scar collagen content. This finding has significant implications for doxycycline's therapeutic potential, as scars are known to have decreased strength compared with healthy skin, and agents that reduce scar burden typically tend to do so at the cost of decreasing scar strength even further.

Consistent with prior reports, doxycycline exhibited a number of off-target effects in tissue.<sup>4</sup> For instance, there are several studies that suggest that doxycycline has anti-inflammatory properties.<sup>27–29</sup> Interestingly, our data do not demonstrate that any significant change occurs in the number of inflammatory cells in doxycycline-treated wounds. In the past, increased inflammation has been linked to delays in wound healing<sup>30</sup> and issues with chronic open wounds.<sup>31</sup> In our study, despite the trend toward increased inflammatory cell recruitment, doxycycline did not impair wound healing. Our data also indicate that doxycycline's favorable effects on scar collagen may be mediated at least in part by decreasing the scarring fibroblast (EPF) cell population.

Most importantly, the vulnerary effects of doxycycline have immediate therapeutic potential for human patients. Several specific findings have important clinical implications. Our data suggest superiority of 2mg/mL doxycycline treatment over other concentrations, though further study will be required to determine optimal human dosing, as well as dosing for different formulations of doxycycline. Our data also strongly suggest a narrow therapeutic window for administration of doxycycline, such that administration must occur within 12 hours following injury to achieve reduced scar thickness, and optimal dosing exists at 2mg/mL and must not exceed 20 mg/mL.

There are several reports which indicate that doxycycline may act as a collagenase inhibitor.<sup>32–34</sup> This was not examined within this study but may ultimately explain the mechanism of reduced skin scarring with local doxycycline treatment. Specifically, collagenases are known to be excreted by fibroblasts and local inflammatory cells. Their function is primarily to break down and aid in the maturation of scar collagen. Early in wound healing, EPFs deposit type III collagen and immature type I collagen, both of which exhibit green birefringence. As the wound matures, type III collagen is gradually replaced by type I collagen, and over time the fibers are aligned in a parallel fashion prior to initiating wound contraction.<sup>22</sup> Collagenases play an important role in this process, by breaking down scar collagens to facilitate wound maturation.<sup>35,36</sup> To expand upon this knowledge, we believe future experiments should target the level of collagenases both in the tissue and within *engrailed1* fibroblasts post wounding and doxycycline treatment. Based on the literature available to date, a biological link between collagenase inhibition and fibroblast apoptosis does not exist. Thus, we cannot explain based on our experiments or available literature how doxycycline treated wounds have both reduced scar collagen and reduced numbers of scar forming fibroblasts.

Interestingly, we did not find a similar effect with 2 other commonly used tetracycline antibiotics. When minocycline and tetracycline were tested at equivalent doses, the opposite impact on skin scarring was observed. Specifically, scar thickness increased with local treatment with tetracycline and minocycline, in contrast to the decrease observed with doxycycline. Studies on the vulnerary capacity of minocycline and tetracycline suggest that

they should also function as collagenase inhibitors.<sup>37,38</sup> However, it is possible that the effects of these other antibiotics on scarring are also dose dependent, and to definitively conclude that other tetracycline class antibiotics do not share the same vulnerary capabilities as doxycycline, dose testing similar to our initial experiment would need to be completed.

The finding that oral dosing of doxycycline did not significantly affect scarring indicates that enteral delivery may not attain a sufficient tissue concentration to permit doxycycline's antiscarring effects. However, we did not perform serum and tissue doxycycline levels, which would improve the strength of this conclusion. Additionally, intraperitoneal injections would have resulted in a physiologic pulse of doxycycline more comparable to what is seen in human enteral dosing than the method of delivering doxycycline in drinking water used in this study. Both intraperitoneal injections coupled with serum and tissue doxycycline level testing would validate our conclusion that doxycycline's vulnerary capacity appears to be specific to local administration. Alternatively, we could have performed PO dose testing using pulses or limited exposure, as we are uncertain whether constant exposure to doxycycline will have the same impact on wound healing.

Finally, doxycycline is well tolerated and has a longstanding safety profile in clinical patients. However, it has yet to be incorporated into wound healing and antiscarring pharmaceuticals and products. For these reasons, we are enthusiastic about rapid translation to human trials. Through the publication of this paper, we hope to generate demand and support among our surgical colleagues for the development of doxycycline containing antiscarring therapies. We hope this can encourage our pharmaceutical partners and translational science colleagues to develop novel products harnessing doxycycline as a vulnerary agent. In the future, we envision the development of novel therapeutics such as combined lidocaine-doxycycline formulations, topical acne treatments, and petroleum jelly-doxycycline formulations to permit favorable wound healing after surgical incisions and injuries acquired at home.

## Supplementary Material

Refer to Web version on PubMed Central for supplementary material.

## ACKNOWLEDGMENTS

The authors thank Reinhold H. Dauskardt for the use of a microtester. The authors also thank Charles Chan, Patricia Lovelace, and Stephen Weber for their help developing a complex hematopoietic lineage sorting profile.

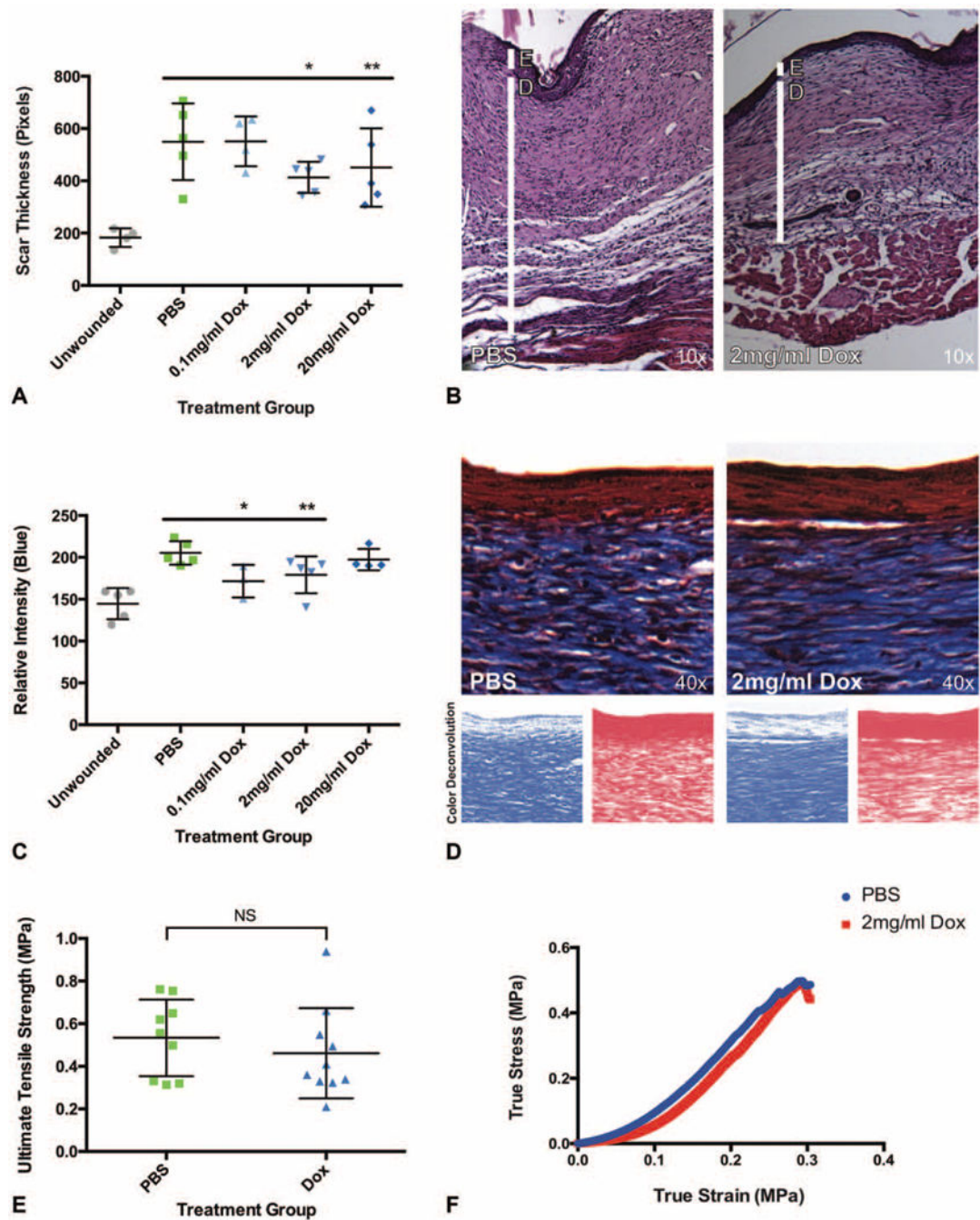
This work was supported by the Hagey Laboratory for Pediatric Regenerative Medicine and the Glenn/Olivier Fund to M.T.L. A FACS Aria II used to generate the immune cell profile was purchased by the Stanford University Lorry I. Lokey Stem Cell Research Building and the Stanford Institute of Stem Cell Biology and Regenerative Medicine using an NIH S10 Shared Instrumentation Grant (1S10RR02933801). A.L.M. was supported by the Society of University Surgeons Research Fellowship Award and the Stanford Tissue and Transplant Engineering Center of Excellence Fellowship Award.

Experiments were performed per Stanford University and the Institutional Animal Care and Use Committee guidelines.

## REFERENCES

1. Sen CK, Gordillo GM, Roy S, et al. Human skin wounds: a major and snowballing threat to public health and the economy. *Wound Repair Regen.* 2009;17:763–771. [PubMed: 19903300]
2. Gauglitz GG, Korting HC, Pavicic T, et al. Hypertrophic scarring and keloids: pathomechanisms and current and emerging treatment strategies. *Mol Med.* 2011;17:113–125. [PubMed: 20927486]
3. Brown BC, McKenna SP, Siddhi K, et al. The hidden cost of skin scars: quality of life after skin scarring. *J Plast Reconstr Aesthet Surg.* 2008;61:1049–1058. [PubMed: 18617450]
4. Henehan M, Montuno M, De Benedetto A. Doxycycline as an anti-inflammatory agent: updates in dermatology. *J Eur Acad Dermatol Venereol.* 2017;31:1800–1808. [PubMed: 28516469]
5. Smith GN Jr, Mickler EA, Hasty KA, et al. Specificity of inhibition of matrix metalloproteinase activity by doxycycline: relationship to structure of the enzyme. *Arthritis Rheum.* 1999;42:1140–1146. [PubMed: 10366106]
6. Li DQ, Shang TY, Kim HS, et al. Regulated expression of collagenases MMP-1, -8, and -13 and stromelysins MMP-3, -10, and -11 by human corneal epithelial cells. *Invest Ophthalmol Vis Sci.* 2003;44:2928–2936. [PubMed: 12824233]
7. Choi DH, Moon IS, Choi BK, et al. Effects of sub-antimicrobial dose doxycycline therapy on crevicular fluid MMP-8, and gingival tissue MMP-9, TIMP-1 and IL-6 levels in chronic periodontitis. *J Periodontal Res.* 2004;39:20–26. [PubMed: 14687223]
8. Gomes JR, Omar NF, Neves JDS, et al. Doxycycline reduces the expression and activity of matrix metalloproteinase-2 in the periodontal ligament of the rat incisor without altering the eruption process. *J Periodontal Res.* 2017;52:353–359. [PubMed: 27417412]
9. Tharappel JC, Ramineni SK, Reynolds D, et al. Doxycycline impacts hernia repair outcomes. *J Surg Res.* 2013;184:699–704. [PubMed: 23830364]
10. Ishikawa C, Tsuda T, Konishi H, et al. Tetracyclines modulate protease-activated receptor 2-mediated proinflammatory reactions in epidermal keratinocytes. *Antimicrob Agents Chemother.* 2009;53:1760–1765. [PubMed: 19258275]
11. Esterly NB, Koransky JS, Furey NL, et al. Neutrophil chemotaxis in patients with acne receiving oral tetracycline therapy. *Arch Dermatol.* 1984;120:1308–1313. [PubMed: 6237616]
12. Crocco E, Pascini M, Suzuki N, et al. Minocycline for the treatment of cutaneous silicone granulomas: a case report. *J Cosmet Laser Ther.* 2016;18:48–49. [PubMed: 26073116]
13. Galiano RD, Michaels Jt, Dobryansky M, et al. Quantitative and reproducible murine model of excisional wound healing. *Wound Repair Regen.* 2004;12: 485–492. [PubMed: 15260814]
14. Hu MS, Walmsley GG, Barnes LA, et al. Delivery of monocyte lineage cells in a biomimetic scaffold enhances tissue repair. *JCI Insight.* 2017;2 Epub ahead of print.
15. Rustad KC, Wong VW, Sorkin M, et al. Enhancement of mesenchymal stem cell angiogenic capacity and stemness by a biomimetic hydrogel scaffold. *Biomaterials.* 2012;33:80–90. [PubMed: 21963148]
16. Rinkevich Y, Walmsley GG, Hu MS, et al. Skin fibrosis. Identification and isolation of a dermal lineage with intrinsic fibrogenic potential. *Science.* 2015;348 aaa2151.
17. Kim S, Thiessen PA, Bolton EE, et al. PubChem substance and compound databases. *Nucleic Acids Res.* 2016;44:D1202–D1213. [PubMed: 26400175]
18. Cunha BA, Comer JB, Jonas M. The tetracyclines. *Med Clin North Am.* 1982;66:293–302. [PubMed: 7038336]
19. Supp AP, Neely AN, Supp DM, et al. Evaluation of cytotoxicity and antimicrobial activity of Acticoat Burn Dressing for management of microbial contamination in cultured skin substitutes grafted to athymic mice. *J Burn Care Rehabil.* 2005;26:238–246. [PubMed: 15879745]
20. Hershman MJ, Pietsch JD, Trachtenberg L, et al. Protective effects of recombinant human tumour necrosis factor alpha and interferon gamma against surgically simulated wound infection in mice. *Br J Surg.* 1989;76:1282–1286. [PubMed: 2514003]
21. Agostinho Hunt AM, Gibson JA, Larrivee CL, et al. A bioluminescent *Pseudomonas aeruginosa* wound model reveals increased mortality of type 1 diabetic mice to biofilm infection. *J Wound Care.* 2017;26:S24–S33. [PubMed: 28704171]

22. Moore AL, Marshall CD, Barnes LA, et al. Scarless wound healing: transitioning from fetal research to regenerative healing. *Wiley Interdiscip Rev Dev Biol.* 2018;7 e309.
23. Lattouf R, Younes R, Lutomski D, et al. Picosirius red staining: a useful tool to appraise collagen networks in normal and pathological tissues. *J Histochem Cytochem.* 2014;62:751–758. [PubMed: 25023614]
24. Ko SH, Nauta A, Morrison SD, et al. Antimycotic ciclopirox olamine in the diabetic environment promotes angiogenesis and enhances wound healing. *PLoS One.* 2011;6:e27844. [PubMed: 22125629]
25. Steinbrech DS, Longaker MT, Mehrara BJ, et al. Fibroblast response to hypoxia: the relationship between angiogenesis and matrix regulation. *J Surg Res.* 1999;84:127–133. [PubMed: 10357908]
26. Mah W, Jiang G, Olver D, et al. Elevated CD26 expression by skin fibroblasts distinguishes a profibrotic phenotype involved in scar formation compared to gingival fibroblasts. *Am J Pathol.* 2017;187:1717–1735. [PubMed: 28641076]
27. Payne JB, Golub LM, Stoner JA, et al. The effect of subantimicrobial-dose-doxycycline periodontal therapy on serum biomarkers of systemic inflammation: a randomized, double-masked, placebo-controlled clinical trial. *J Am Dent Assoc.* 2011;142:262–273. [PubMed: 21357860]
28. Choi JS, Kim JM, Kim JW, et al. Prevention of tracheal inflammation and fibrosis using nitinol stent coated with doxycycline. *Laryngoscope.* 2017;128:1558–1563. [PubMed: 29266274]
29. Bian F, Pelegrino FS, Henriksson JT, et al. Differential effects of dexamethasone and doxycycline on inflammation and MMP production in murine alkali-burned corneas associated with dry eye. *Ocul Surf.* 2016;14:242–254. [PubMed: 26772899]
30. Hart J. Inflammation2: its role in the healing of chronic wounds. *J Wound Care.* 2002;11:245–249. [PubMed: 12192842]
31. Zhao G, Usui ML, Lippman SI, et al. Biofilms and inflammation in chronic wounds. *Adv Wound Care (New Rochelle).* 2013;2:389–399. [PubMed: 24527355]
32. Wang S, Liu C, Liu X, et al. Effects of matrix metalloproteinase inhibitor doxycycline and CD147 antagonist peptide-9 on gallbladder carcinoma cell lines. *Tumour Biol.* 2017;39 [1010428317718192](https://doi.org/10.100428317718192).
33. Lam-Franco L, Perfecto-Avalos Y, Patiño-Ramírez BE, et al. IL-1 $\alpha$  and MMP-9 tear levels of patients with active ocular rosacea before and after treatment with systemic azithromycin or doxycycline. *Ophthalmic Res.* 2018;60: 109–114. [PubMed: 29874670]
34. Kimmitt BA, Moore GE, Stiles J. Comparison of the efficacy of various concentrations and combinations of serum, ethylenediaminetetraacetic acid, tetracycline, doxycycline, minocycline, and N-acetylcysteine for inhibition of collagenase activity in an in vitro corneal degradation model. *Am J Vet Res.* 2018;79:555–561. [PubMed: 29688786]
35. Gurtner GC, Werner S, Barrandon Y, et al. Wound repair and regeneration. *Nature.* 2008;453:314–321. [PubMed: 18480812]
36. Amar S, Smith L, Fields GB. Matrix metalloproteinase collagenolysis in health and disease. *Biochim Biophys Acta Mol Cell Res.* 2017;1864(11 pt A): 1940–1951. [PubMed: 28456643]
37. Ghangurde AA, Ganji KK, Bhongade ML, et al. Role of chemically modified tetracyclines in the management of periodontal diseases: a review. *Drug Res (Stuttg).* 2017;67:258–265. [PubMed: 28268238]
38. Golub LM, Lee HM, Ryan ME, et al. Tetracyclines inhibit connective tissue breakdown by multiple non-antimicrobial mechanisms. *Adv Dent Res.* 1998;12:12–26. [PubMed: 9972117]

**FIGURE 1.**

Doxycycline improves wound thickness without sacrificing tensile strength. A, Scar thickness is significantly reduced in 2 and 20 mg/mL doxycycline treated wounds (n = 10 wounds per group, \* $P < 0.0001$ , \*\* $P = 0.0023$ ). B, Representative histology of scar treated with vehicle (PBS, left panel) and 2 mg/mL doxycycline (right panel) by hematoxylin and eosin stain. E, Epidermis; D, dermis. C, Relative scar collagen is significantly reduced in 0.1 and 2 mg/mL doxycycline groups as measured by Masson trichrome stain (n = 10 wounds, \* $P = 0.0357$ , \*\* $P = 0.0317$ ). D, Representative histology of scar treated with vehicle (PBS,

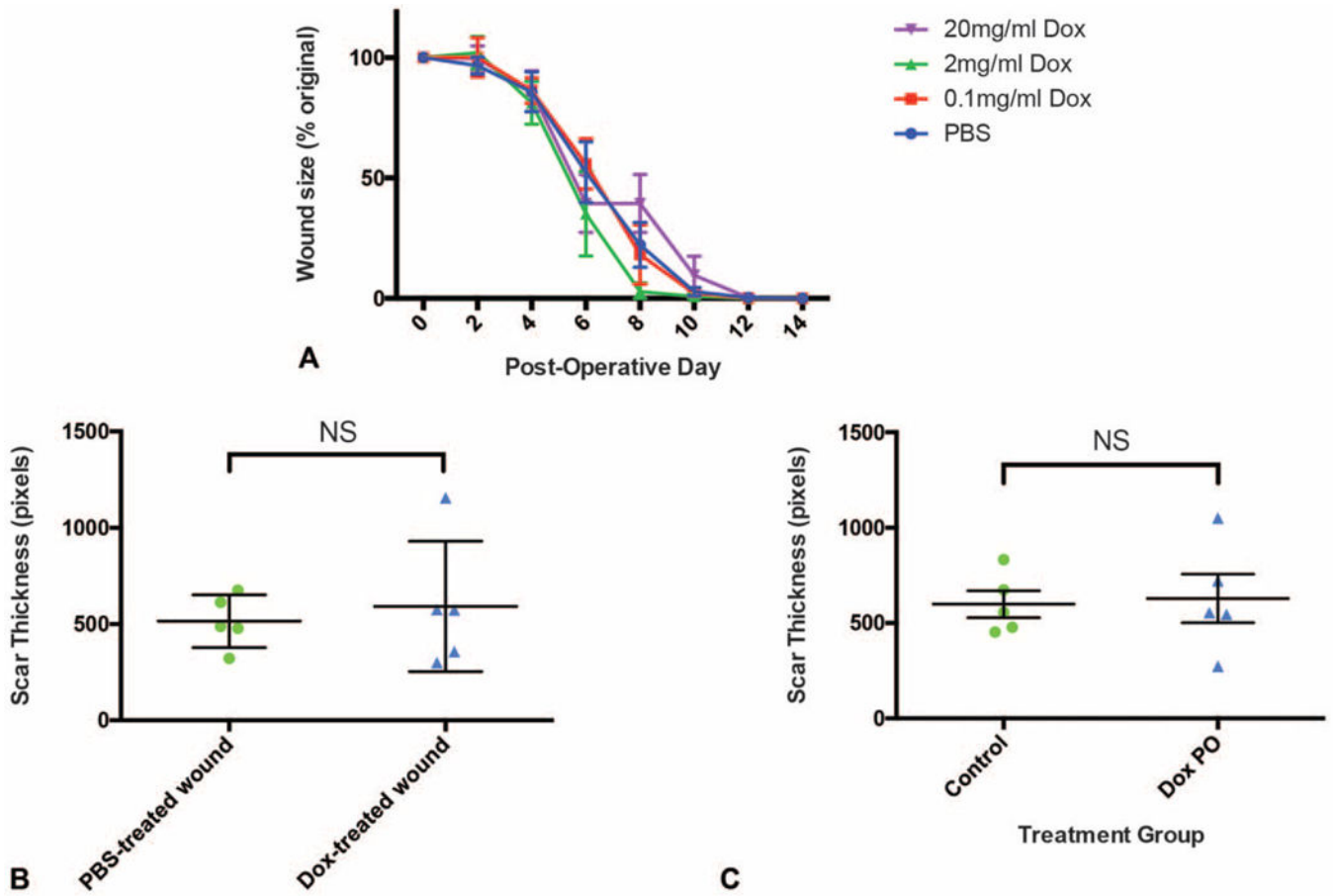
left) and 2 mg/mL doxycycline (right) using Masson trichrome stain (top panels), with representative color deconvolution of the above image (blue deconvolution, bottom left panels; red deconvolution, bottom right panels). E, Tensile strength is not significantly different between vehicle and 2 mg/mL doxycycline (Dox) treatment groups ( $n = 10$  wounds,  $P = 0.4376$ ). F, Representative tensile strength curves for PBS control and 2 mg/mL doxycycline treatment. A, C, Results depicted as mean per animal  $\pm$  SEM. E, Tensile strength depicted as individual wound strength measurements  $\pm$  SEM. \*, \*\*, denotes statistical significance; NS, not statistically significant.

Author Manuscript

Author Manuscript

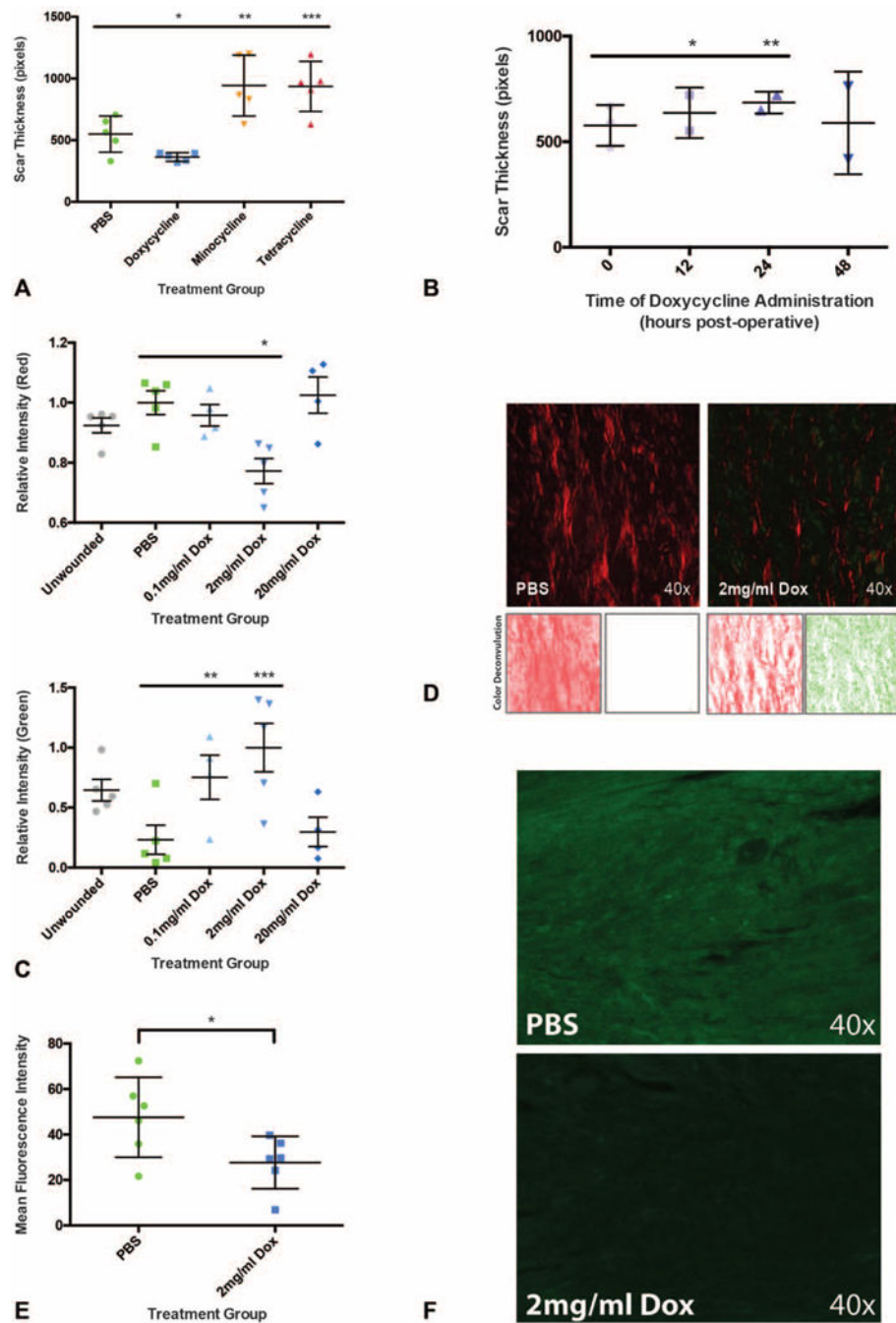
Author Manuscript

Author Manuscript

**FIGURE 2.**

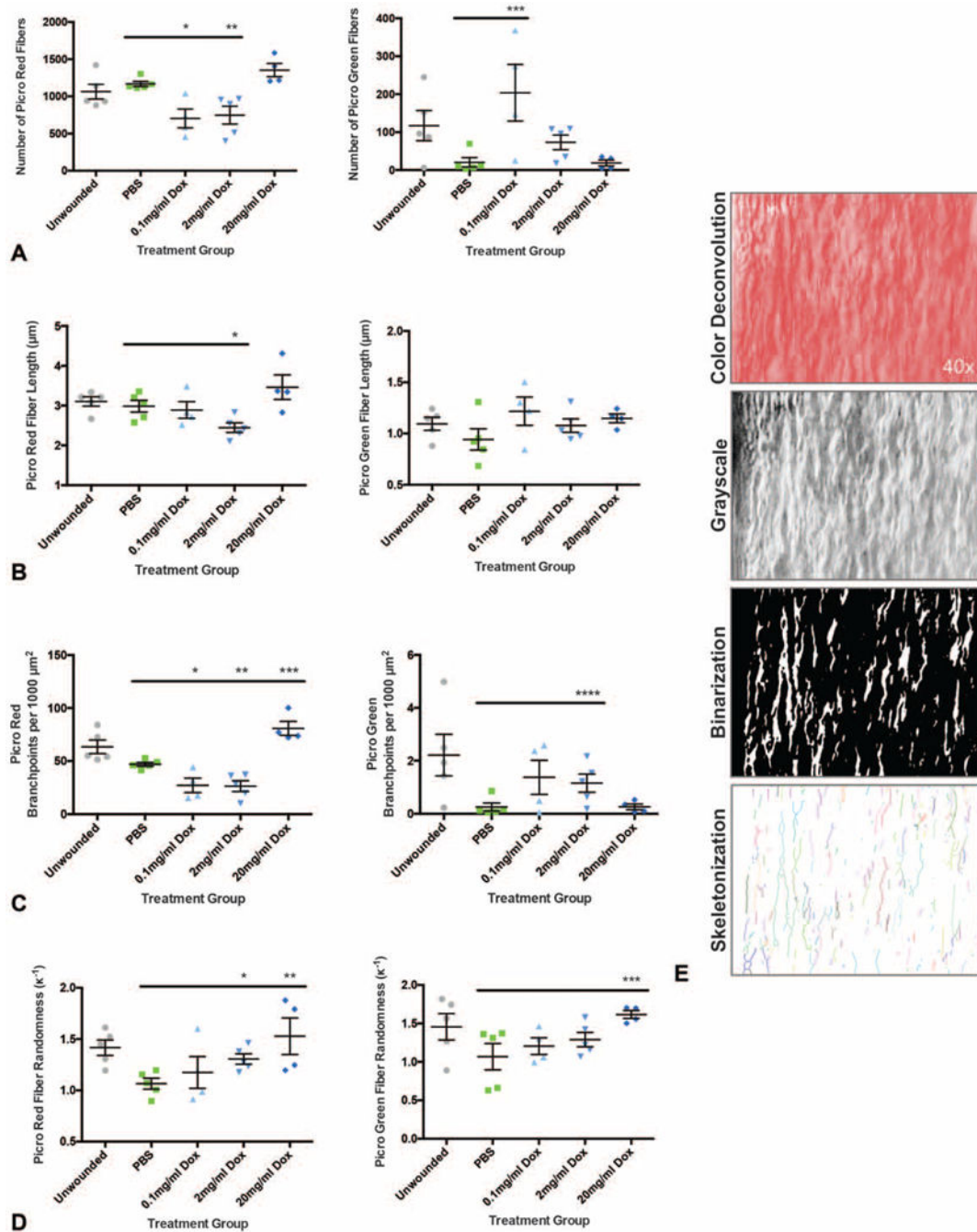
Reduced skin scar thickness by doxycycline treatment depends on local administration and does not delay wound healing. A, Time to wound closure is not adversely influenced by doxycycline administration in 0.1, 2, and 20mg/mL treatment groups compared with PBS controls ( $n = 10$  wounds,  $P > 0.24378$  at all timepoints). B, Treatment of the right wound with 2 mg/mL doxycycline and left wound with PBS in the same mouse led to comparably reduced scar thickness in the left and right wounds ( $n = 5$  animals,  $P = 0.6257$ ). C, Oral administration of 2 mg/mL doxycycline via drinking water did not result in reduced scar thickness ( $n = 10$  wounds,  $P = 0.3006$ ). Control, PBS injection; Dox PO, oral doxycycline. Results depicted as mean ((A), per group per day; (B), per wound; (C), per mouse)  $\pm$  SEM. NS indicates not statistically significant.



**FIGURE 3.**

The ability to reduce scar thickness is unique to doxycycline and depends on early administration. A, Improvement in scar thickness is limited to doxycycline ( $n = 10$  wounds,  $*P < 0.0001$ ). Other tetracycline antibiotics (minocycline, tetracycline) significantly thicken dorsal skin scars compared with control treatment ( $n = 10$  wounds,  $**P < 0.0001$ ,  $***P < 0.0001$ ). B, Delaying doxycycline injection to 12 and 24 hours postoperatively results in increasing scar thickness ( $n = 4$  wounds,  $*P = 0.0066$ ,  $**P < 0.0001$ ). A nonsignificant increase in scar thickness but increased variability is seen when doxycycline administration

is delayed to 48 hours postoperatively ( $n = 4$  wounds,  $P = 0.8848$ , T0 h SEM = 12.37, T48 h SEM = 29.03). C, A decrease in Picro Red fibers (top panel) and increase in Picro Green fibers (bottom panel) is seen in the 2 mg/mL group ( $n = 10$  wounds,  $*P = 0.0042$ ,  $**P = 0.0441$ ,  $***P = 0.0114$ ). D, Representative Picrosirius staining for wounds treated with PBS (upper left panel) and 2 mg/mL doxycycline (upper right panel), with representative color deconvolution of Picrosirius images (red deconvolution, bottom left panels; green deconvolution, bottom right panels) which allowed for the separate measurement of Picro Red and Picro Green collagen fibers. E, Collagen I immunostaining is significantly reduced in the 2 mg/mL group compared with control ( $n = 6$  wounds,  $*P = 0.0430$ ). F, Representative anti-collagen I (green) immunostaining in PBS (top panel) and 2 mg/mL doxycycline (bottom panel) groups. \*, \*\*, \*\*\*, denotes statistical significance. Results depicted as mean per animal  $\pm$  SEM.

**FIGURE 4.**

Analysis of collagen fiber orientation reveals a favorable phenotype in doxycycline treated skin scars. A, Picro Red fiber number (left panel) is significantly reduced in the 0.1 and 2 mg/mL treatment groups (left panel; n = 10 wounds, \* $P = 0.0054$ , \*\* $P = 0.0098$ ) and Picro Green fiber number is significantly increased in the 0.1 mg/mL group (right panel; n = 10 wounds, \*\*\* $P = 0.0292$ ). B, Picro Red fiber length (left panel) is significantly reduced in the 2 mg/mL group (n = 10 wounds, \* $P = 0.0226$ ). C, Picro Red fiber branching (left panel) is significantly decreased in the 0.1 and 2 mg/mL groups but increased with 20 mg/mL

treatment (n = 10 wounds, \* $P=0.0159$ , \*\* $P=0.0053$ , \*\*\* $P=0.0009$ ). Picro Green fibers also have increased branching (right panel; n = 10 wounds, \*\*\*\* $P=0.0444$ ). D, Fiber randomness is increased in Picro Red fibers (left panel; n = 10 wounds, \* $P=0.0115$ , \*\* $P=0.0282$ , left panel) and Picro Green fibers (right panel; n = 10 wounds, \*\*\* $P=0.0289$ ). E, Representation of image deconvolution for analysis, including color deconvolution, conversion to grayscale, image binarization, and skeletonization. \*, \*\*, \*\*\*, \*\*\*\*, denotes statistical significance. Results depicted as mean per animal  $\pm$  SEM.

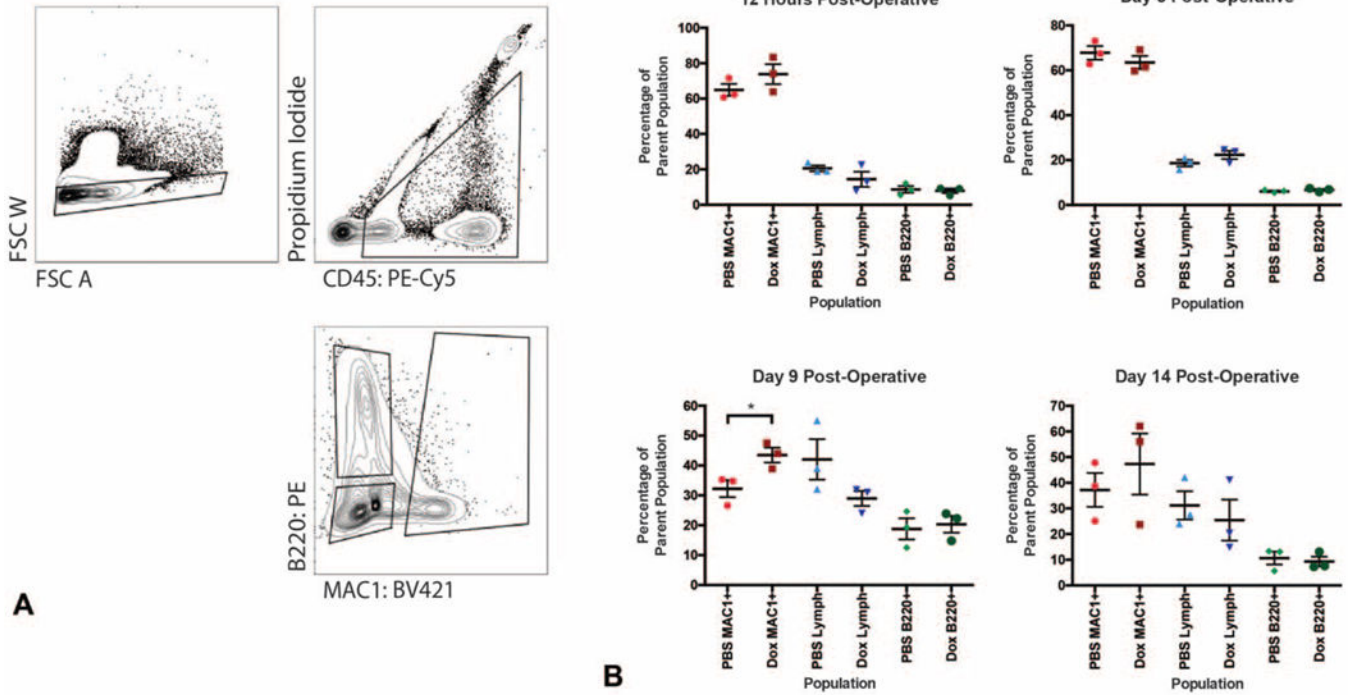


**FIGURE 5.** FACS analysis of inflammatory cell populations within doxycycline treated wounds over time. A, FACS gating strategy for the MAC1+, B220+, and double negative populations. B, Effects of doxycycline on relative populations of macrophage (MAC1+), B cell (B220+), and lymphocyte (double negative, Lymph) cell populations in the wounds at 12 hours (top left panel), 5 (top right), 9 (bottom left), and 14 days (bottom right) postinjury. Macrophages are significantly increased with doxycycline treatment at day 9 postinjury (n = 6 wounds, \**P* = 0.0407). \*, denotes statistical significance. Results depicted as mean per animal ± SEM.

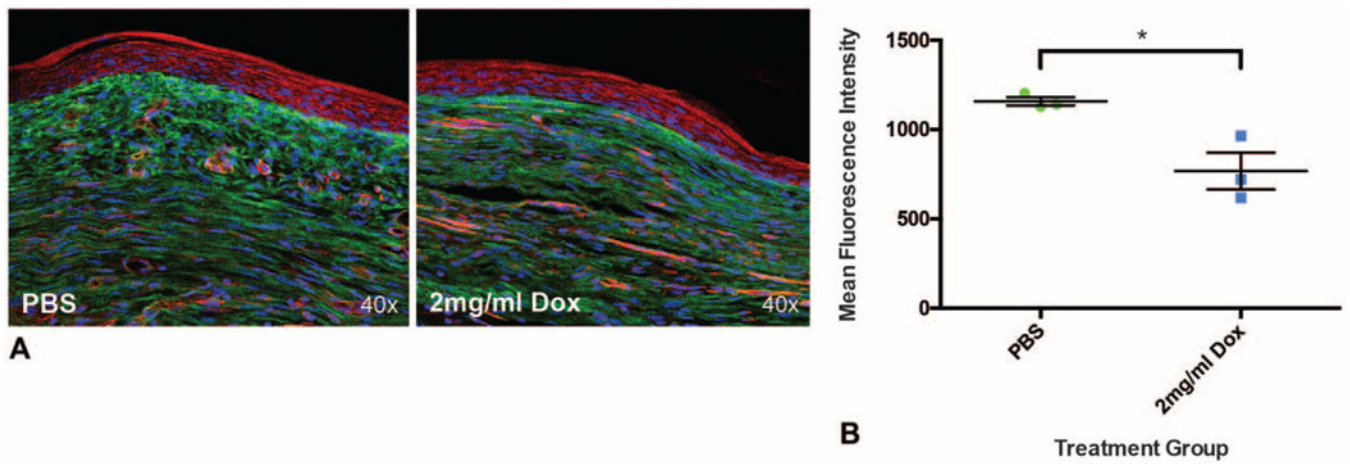


**FIGURE 6.** Scarring fibroblasts are significantly reduced in wounds treated with doxycycline. A, Representative histology of *En1<sup>Cre/+</sup>;Rosa26<sup>mTmG/+</sup>* skin wounds treated with PBS (left panel) and 2mg/mL doxycycline (right panel). B, *Engrailed1* positive fibroblasts (EPFs) in wounds are significantly reduced with doxycycline treatment (n = 6 wounds, \**P* = 0.0005). \*, denotes statistical significance. Results depicted as mean per animal ± SEM.